GABBR1 monoallelic *de novo* variants linked to neurodevelopmental delay and epilepsy

Authors

Maria Lucia Cediel, Michal Stawarski, Xavier Blanc, ..., Emmanuelle Ranza, Bernhard Bettler, Stylianos E. Antonarakis

Correspondence

stylianos.antonarakis@medigenome.ch

Pathogenic mutations in the human gene GABBR1 (encoding a protein that forms a receptor in neuronal cells) cause a rare autosomal dominant disorder with neurodevelopmental delay and epilepsy. These findings are important for diagnosis and genetic counseling; in addition, they provide the opportunity for development of new therapies.

Cediel et al., 2022, The American Journal of Human Genetics *109*, 1885–1893
October 6, 2022

https://doi.org/10.1016/j.ajhg.2022.08.010

GABBR1 monoallelic *de novo* variants linked to neurodevelopmental delay and epilepsy

Maria Lucia Cediel,[1,8] Michal Stawarski,[2,8] Xavier Blanc,[1] Lenka Nosková,[3] Martin Magner,[3,4] Konrad Platzer,[5] Janina Gburek-Augustat,[6] Dustin Baldridge,[7] John N. Constantino,[7] Emmanuelle Ranza,[1,9,10] Bernhard Bettler,[2,9,10] and Stylianos E. Antonarakis[1,9,10,*]

Summary

$GABA_B$ receptors are obligatory heterodimers responsible for prolonged neuronal inhibition in the central nervous system. The two receptor subunits are encoded by *GABBR1* and *GABBR2*. Variants in *GABBR2* have been associated with a Rett-like phenotype (MIM: 617903), epileptic encephalopathy (MIM: 617904), and milder forms of developmental delay with absence epilepsy. To date, however, no phenotypes associated with pathogenic variants of *GABBR1* have been established. Through GeneMatcher, we have ascertained four individuals who each have a monoallelic *GABBR1 de novo* non-synonymous variant; these individuals exhibit motor and/or language delay, ranging from mild to severe, and in one case, epilepsy. Further phenotypic features include varying degrees of intellectual disability, learning difficulties, autism, ADHD, ODD, sleep disorders, and muscular hypotonia. We functionally characterized the four *de novo GABBR1* variants, p.Glu368Asp, p.Ala397Val, p.Ala535Thr, and p.Gly673Asp, in transfected HEK293 cells. GABA fails to efficiently activate the variant receptors, most likely leading to an increase in the excitation/inhibition balance in the central nervous system. Variant p.Gly673Asp in transmembrane domain 3 (TMD3) renders the receptor completely inactive, consistent with failure of the receptor to reach the cell surface. p.Glu368Asp is located near the orthosteric binding site and reduces GABA potency and efficacy at the receptor. GABA exhibits normal potency but decreased efficacy at the p.Ala397Val and p.Ala535Thr variants. Functional characterization of *GABBR1*-related variants provides a rationale for understanding the severity of disease phenotypes and points to possible therapeutic strategies.

Introduction

The major inhibitory neurotransmitter in the central nervous system is γ-aminobutyric acid (GABA). GABA acts at ionotropic $GABA_A$/$GABA_C$ receptors and metabotropic $GABA_B$ receptors.[1] $GABA_B$ receptors are G protein-coupled receptors that reduce cAMP levels and regulate Kir3-type potassium and voltage-sensitive calcium channels.[1,2] $GABA_B$ receptors are expressed throughout the brain in glial cells and neurons. In neurons, they act at pre- and postsynaptic sites, where they inhibit neurotransmitter release and generate the late phase of inhibitory postsynaptic potentials.[2] $GABA_B$ receptors in microglia have been implicated in the sculpting of inhibitory circuits.[3] In astrocytes, $GABA_B$ receptors mediate calcium elevations and influence hippocampal theta and gamma oscillations.[4,5]

$GABA_B$ receptors are obligatory heterodimers made up of a GB1a or GB1b with a GB2 subunit, which are encoded by the *GABBR1* (MIM: 603540) and *GABBR2* genes (MIM: 607340).[2] GB1a and GB1b are subunit variants generated by alternative promoter usage. GB1a and GB1b have similar functional and pharmacological properties when expressed in heterologous cells.[2] GB1 and GB2 subunits share 54% amino acid sequence and 35% nucleotide sequence similarity. Heterodimerization of the GB1 and GB2 subunits is necessary for receptor trafficking from the endoplasmic reticulum to the cell surface.[6–9] GB1 and GB2 subunits consist of three domains: (1) an extracellular Venus-fly-trap domain (VFTD) composed of an N-terminal domain (LB1) and a C-terminal domain (LB2), (2) a heptahelical transmembrane domain (7TMD), and (3) a C-terminal intracellular domain.[1,10] The VFTD of the GB1a and GB1b subunits contains the orthosteric binding site while the VTFD on the GB2 subunit is coupling to the G protein. The LB1 and LB2 domains of the GB1 and GB2 VFTD interact with each other to form the extracellular heterodimer interface, which is essential for receptor activation.[1,10]

$GABA_B$ receptor dysfunctions have been implicated in neurological and neurodevelopmental disorders including anxiety, autism, depression, addiction, epilepsy, and cognition[11–14]. *GABBR2* variants are implicated in Rett-like

[1]Medigenome, Swiss Institute of Genomic Medicine, 1207 Geneva, Switzerland; [2]Department of Biomedicine, Pharmazentrum, University of Basel, Klingelbergstrasse 50/70, 4056 Basel, Switzerland; [3]Department of Pediatrics and Inherited Metabolic Disorders, First Faculty of Medicine, Charles University and General University Hospital in Prague, Prague, Czech Republic; [4]Department of Pediatrics, First Faculty of Medicine, Charles University and University Thomayer Hospital in Prague, Prague, Czech Republic; [5]Institute of Human Genetics, University of Leipzig Medical Center, Leipzig, Germany; [6]Division of Neuropaediatrics, Hospital for Children and Adolescents, University Hospital Leipzig, Leipzig, Germany; [7]Washington University in St. Louis, St. Louis, MO, USA
[8]These authors contributed equally
[9]These authors contributed equally
[10]Joint last authors
*Correspondence: stylianos.antonarakis@medigenome.ch
https://doi.org/10.1016/j.ajhg.2022.08.010.

symptoms, epileptic encephalopathy, and severe intellectual disability.[11–14] As $GABA_B$ receptors are obligatory heterodimers, one could expect a similar phenotypic spectrum for pathological variants in *GABBR1*. Indeed, mice lacking the GB1 or GB2 subunits develop similar neurological disorders, including clonic type seizures, but also absence and tonic-clonic seizures as well as hyperactivity, hyperalgesia, and poor memory performance.[15,16] In humans, one study suggested that a *GABBR1* non-coding polymorphic variant is associated with temporal lobe epilepsy, but this finding is controversial.[17,18]

In this study, we report four individuals with heterozygous *GABBR1 de novo* missense variants, all presenting neurodevelopmental motor and/or language delays. Two of the four individuals have varying degrees of intellectual disability, learning difficulties, and a sleep disorder. Two individuals have attention-deficit/hyperactivity disorder (ADHD), and one individual additionally presents with other concomitant psychiatric disorders (autism, borderline personality disorder, oppositional defiant disorder [ODD], social anxiety, and one episode of major depressive disorder [MDD]). One individual is treated for epileptic seizures. Functional analyses reveal that all four variants produce dysfunctional receptors, supporting that these *de novo* variants are pathogenic.

Material and methods

Individuals

Four individuals were evaluated at their respective clinical institutions and the GABBR1 variants were respectively added to the web-based platform GeneMatcher[19] and collected. Each clinic obtained a written consent form to participate in the publication from the legal guardians. The study was performed in accordance with the principles of Swiss Society of Medical Genetics.

Whole-exome sequencing

Each center performed a whole-exome sequencing (WES) in trio (proband and parents). The methodology of each center is provided in the supplemental information.

Functional analysis

A functional characterization of the four *de novo* GB1 subunit variants (p.Glu368Asp, p.Ala397Val, p.Ala535Thr, and p.Gly673Asp)] was carried out in transfected HEK293 cells.

Plasmids and reagents

Human GB1b and GB2 plasmids were used earlier;[20] SRE-FLuc (28) was a gift from M. Choi, Seoul. Mutant GB1b subunits and N-terminally HA-tagged subunits were generated with the Q5 Site-Directed Mutagenesis kit (New England Biolabs, Ipswich, USA). The following primers were used: p.Glu368Asp_For ACTTTTCTATgacACTGA AGCCCGG and p.Glu368Asp_Rev CCCACGATGATTCGGGCA; p.(Ala397Val) was generated with the following mutagenic primers: p.(Ala397Val)_For TGGGTGGTATgttGACAATTGGT and p.(Ala397 Val)_Rev ATGAGGAACCAGACGTAC; p.(Ala535Thr)_For CTCTCG GATGacaTGGACGCTTATC and p.(Ala535Thr)_Rev CCCACGAT GATTCGGGCA; p.(Gly673Asp) _For CCTGGGCCTGgacTTTAGT CTGGGC and p.(Gly673Asp) _Rev AGCCAGAGGCGGGCCTGG (small caps indicate the mutation). The N-terminal HA-tag was inserted with GB1b_HA_For ttatgcgggcggcggcagcTCCCACTCCCCC CATCTCC and GB1b_Rev tccggcacatcatacggataGGCCCACACCG GAGCCAC (small caps indicate HA-tag). GABA and CGP54626 were from Tocris Bioscience (Bristol, England). Anti-HA antibodies (clone 3F10) were from Roche (Basel, Switzerland). Anti-GB1 antibodies (#55051) were from Abcam (Cambridge, UK). Anti-βactin antibodies (#4970) were from Cell Signaling Technology (Danvers, USA). AF568-conjugated anti-rat and AF488-conjugated anti-mouse secondary antibodies were from Invitrogen. HRP-conjugated anti-mouse and anti-rabbit antibodies were from GE Healthcare (Chicago, USA). Poly-L-Lysine was from Sigma (Burlington, USA). The following transfection reagents were used: Lipofectamine 2000 from Invitrogen (Waltham, USA) and PEI from Sigma. The Plasma Membrane Protein Extraction Kit was from Abcam.

Cell surface expression

HEK293 cells were transiently transfected (Lipofectamine 2000, 2:1 ratio) with HA-GB1b and GB2 constructs. 6 h later, cells were detached and plated on PLL-coated glass coverslips in a 24-well plate at a density of 45,000 cells/well. After 2 days, the growth medium was replaced with Opti-MEM-GlutaMAX supplemented with anti-HA antibody (1:1,000) for 1 h. Subsequently, cells were fixed (4% PFA + 4% sucrose, 10 min, RT), permeabilized (PBS + 0.2% Triton X-100), and incubated overnight at 4°C with the anti-GB1 antibody (1:1,000). The following day, cells were washed with 1×PBS and incubated for 90 min at room temperature with AF568 (HA-tag) and AF488-conjugated (anti-GB1) secondary antibodies (1:500). Imaging was performed on Zeiss LSM880 confocal microscope with a PLAN APO 63× objective. Samples were excited at 488 and 555 nm. Image processing and analysis was done in Fiji (ImageJ). Maximum projection images were generated from *Z* stacks, and average fluorescence intensity was measured in regions of interest (ROIs) encompassing individual cells. We used ROIs of the same shape to obtain background values for the same imaging channel. HA-to-GB1 fluorescence intensity ratios were calculated in Microsoft Excel and exported to GraphPad Prism for statistical analysis. Data were tested for normality with the Shapiro-Wilk normality test and analyzed via Kruskal-Wallis with Dunn's multiple comparison tests.

Protein fractionation

HEK293 cells (single 15 cm diameter Petri dish per GB1 variant) were transiently transfected (PEI, 3:1 ratio, 40 μg total DNA) with plasmids encoding GB1b and GB2. After 24 h, cells were harvested and fractionated with the Plasma Membrane Protein Extraction Kit according to the manufacturer's protocol. Cellular fractions were probed with anti-GB1 (1:300) and anti-βactin (1:1,000) antibodies. Immunoblots were scanned with Vilber Fusion FX camera system. Densitometric analysis was done in Fiji.

SRE-luciferase accumulation assay

HEK293 cells stably expressing $G\alpha_{qi}$ were transiently transfected with WT or mutant GB1b, GB2, and SRE-FLuc (Lipofectamine 2000, 2:1 ratio, 4 μg total DNA). In variant and WT receptor co-expression experiments, equal amounts DNA encoding WT and mutant GB1b were used. Transfected cells were seeded into 96-well microplates (Greiner Bio-One) at a density of 70,000 cells/well. After 24 h, the culture medium was replaced with Opti-MEM-GlutaMAX. GB1b/2 receptors were activated with various concentrations of GABA (10, 50, 100, 500 nM; 1, 5, 10, 50, 100, 500 μM; 1, 5, 10 mM) for 6 h. FLuc activity in lysed cells was measured via the Dual-Luciferase Assay Kit (Promega) with a Spark microplate reader. Luminescence signals were adjusted by subtracting the luminescence obtained when expressing

SRE-FLuc fusion proteins alone. For CGP54626 dose response assays, the culture medium was replaced with Opti-MEM-GlutaMAX + 10 μM or 100 μM GABA. GB1b/2 receptors were blocked with various concentrations of CGP54626 (1, 5, 10, 50, 100, 500 nM; 1, 5, 10, 50, 100 μM) or treated with the same amount of vehicle (DMSO) for 6 h. Data were analyzed and plotted in GraphPad Prism 8. Dose response curves were fitted to the raw data. Curve parameters (tonic activity, Emax, EC50, IC50) were tested for normal distribution and analyzed with Kruskal-Wallis or ANOVA. Appropriate corrections were made in cases where SD were significantly different (Brown-Forsythe test for ANOVA and F-test for t test).

Results

Identification of *GABBR1* variants

Individual 1 carries a heterozygous *de novo* missense p.Ala535Thr variant in *GABBR1* (RefSeq accession number GenBank: NM_001470.4; hg19). Sanger sequencing confirmed its absence in the proband's parents. The variant is absent from gnomAD v.2.1.1 and from BRAVO databases.[21,22] The codon is conserved and the variant is predicted as deleterious by SIFT, Mutation Taster, and Polyphen-2 (Table 1). The variant is localized in the linker between the VFTD and TMD1 of the GB1 subunit (Figure 1A). Using Genematcher, we identified three other individuals carrying heterozygous *de novo* missense *GABBR1* variants: p.Gly673Asp, p.Glu368Asp, and p.Ala397Val. All three variants are absent from gnomAD and predicted as deleterious by the SIFT, Mutation Taster, and Polyphen-2 (Table 1). The variant p.Gly673Asp is located in TMD3 of the GB1 subunit. The p.Glu368Asp and p.Ala397Val variants are located in the VFTD containing the orthosteric GABA-binding site (Figure 1A). All of these codons were well conserved in evolution (Figure S1).

Clinical description of the GABBR1 variant carriers

Individual 1 (GABBR1 p.Ala535Thr) is a 30-month-old female with normal weight and height parameters (weight P25–50, height P50–75), known for neurodevelopmental delays of both motor and language skills. She sat unsupported at 12 months, crawled between 13 and 14 months, and walked at 17 months. She presented poor functional use of her hands and started to self-feed at 27 months. She began babbling, then regressed to no sounds. To date, she presents a significant speech delay with no words except "mama" and communicates through non-verbal language. She presents stereotypical movements of the hands, fingers, and feet and is noted for repetitive circular movements of the tongue as well as diurnal and nocturnal bruxism. Further, she presents a particular intense and "sticky" gaze. She shows axial hypotonia and peripheral hypertonia. There is no history of epilepsy. She suffers from constipation that requires medication and from periodic fever without focus since 12 months of age.

Individual 2 (GABBR1 p.Glu368Asp) is a 4-and-a-half-year-old female with normal weight and height parameters (weight at P25–50, height P10–25), presenting morphological particularities including long philtrum, hinted epicanthus, broad nasal root, clinodactyly of the fifth fingers of both hands, and hypoplasia of the teeth. She has a profound psychomotor and language delay. Opposition of the thumb was acquired around 9 months, she sat independently at 30 months, crawled at 36 months, and currently has no independent gait. She presents poor functional use of her hands (she is fed by her parents). With regard to language, she is nonverbal. She presents stereotypical movements consisting of periodic flapping of the feet. She shows combined axial and peripheral hypotonia. Further, at the neurological level, she presents five episodes of prolonged generalized seizures with conscious disorder and hypoxia during a febrile state. A brain MRI was performed at age 4 that showed a progressive cerebellar atrophy with no changes in the white matter or in the cortex. The electroencephalogram (EEG) revealed monomorphic activity with generalized slow SW (spike-wave) complexes, some with clinical correlate of absence seizures. She is treated with levetiracetam with a positive medical response. She presents with a severe intellectual disability, along with severe learning difficulties and sleep difficulties. With regard to other visceral particularities, at the ocular level she has an optic nerve hypoplasia, cortical visual disorders, nystagmus, and hypermetropia and a scoliosis at the osteo-muscular level.

Individual 3 (GABBR1 p.Ala397Val) is a 13-year-old male with neurodevelopmental delay; he walked independently at 36 months and also presented language delay. Currently, he speaks in short sentences with a limited vocabulary and problems with articulation and grammar. At a younger age, he presented with repetitive wheel-spinning, which is currently resolved. He has a mild intellectual disability (IQ at 58) and moderate learning difficulties. Further, he has an ADHD, encopresis, and sleeping difficulties. There is no notion of epilepsy, and an MRI performed at 2 years of age was normal.

Individual 4 (GABBR1 p.Gly673Asp) is a 17-year-old young woman of average weight and height (P50–75 and P10–25, respectively) with diagnoses of autism spectrum disorder, ADHD, borderline personality disorder, opposition defiant disorder, and social anxiety and one episode of major depressive disorder. She has no intellectual disability, but her autism is severe with extremely rigid thinking and profound defects in social motivation, although she is highly capable of social communication and exchange. Earlier in life, she had significant receptive language delay and moderate expressive speech delay with normal motor milestones (sitting at 7 months and walking at 17 months). At present, her language is fluent but with some pressured speech and fragmentation of flow of expressed ideas. She continues to have anger fits and crying attacks, and she has significant daytime sleepiness. She also has constipation, mood-associated headaches, as well as acne vulgaris, xerosis cutis, multiple melanocytic nevi, and nail dystrophy. She displays congenital

Table 1. *In silico* prediction and conservation of the four *GABBR1* variants

	Individual 1, c.1603G>A (p.Ala535Thr) (GenBank: NM_001470.4)	Individual 2, c.1104G>C (p.Glu368Asp) (GenBank: NM_001470.4)	Individual 3, c.1190C>T (p.Ala397Val) (GenBank: NM_001470.4)	Individual 4, c.2018G>A (p.Gly673Asp) (GenBank: NM_001470.4)
Variant in hg19	chr6: 29580355C>T	chr6: 29589556C>G	chr6: 29589011G>A	chr6: 29574970C>T
Prediction Tools				
gnomAD (non-TOPMed)	absent in 244,660 alleles	absent in 244,844 alleles	absent in 240,972 alleles	absent in 244,834 alleles
BRAVO	absent in 264,690 alleles	absent in 264,690 alleles	absent in 264,690 alleles	absent in 264,690 alleles
CADD	29	23.3	29.4	26.4
SIFT	Deleterious	deleterious	deleterious	deleterious
Mutation Taster	Deleterious	deleterious	deleterious	deleterious
Polyphen-2	Deleterious	deleterious	deleterious	deleterious
Conservation				
GERP NR	5.86	4.55	5.45	4.57
GERP RS	5.86	2.23	5.45	4.57
Codon conservation	Conserved	poor conservation at the nucleotide level, conserved at amino acid level	conserved	conserved

bilateral anteversion of the femur and a bilateral tight heel chord with knee pain. There have been no known seizures.

A summary of the phenotypes can be found in Table 2.

Functional analysis of *GABBR1* variants

We functionally characterized four *de novo* GABBR1 variants, p.Glu368Asp, p.Ala397Val, p.Ala535Thr, and p.Gly673Asp, in transfected HEK293 cells. These variants localize to (1) the VFTD containing the orthosteric GABA-binding site (p.Glu368Asp, p.Ala397Val), (2) the linker between VFTD and TMD1 (p.Ala535Thr), and (3) TMD3 (p.Gly673Asp) (Figure 1A). We first addressed whether HA-tagged wild-type (WT) and mutant GB1b subunits traffic to the cell surface when co-expressed with GB2. We determined cell surface levels GB1b protein with an HA antibody and total GB1b protein after cell permeabilization with a GB1 antibody (Figure 1B). The percentage of GB1b cell surface expression was calculated as the ratio of surface/total immunofluorescence (Figure 1C). As the ratio distribution for some of the receptor variants was not normal (Shapiro-Wilk: HA-p.WT: $p = 0.9752$, HA-p.Glu368Asp: $p = 0.0535$, HA-p.Ala397Val: $p = 0.0003$, HA-p.Ala535Thr: $p = 0.0024$, and HA-p.Gly673Asp: $p = 0.0119$), non-parametric Kruskal-Wallis and Dunn's multiple comparison tests were used. The data show that receptors assembled with p.Ala397Val and p.Ala535Thr traffic normally to the cell surface while p.Glu368Asp and p.Gly673Asp surface expression is significantly reduced or absent, respectively (Kruskal-Wallis: $p < 0.0001$; Dunn's multiple comparison: WT versus p.Glu368Asp and WT versus p.Gly673Asp $p < 0.0001$; remaining pairwise comparisons are not significantly different). We additionally used cellular fractionation of HEK293 cells transiently expressing WT and variant GBRs to study plasma membrane expression of GB1. The GB1 cell surface/total ratios from the fractionation experiments (Figure 1D) are in good agreement with the ratios determined in immunohistochemistry experiments (Figure 1C). Importantly, the fractionation experiments yield the same rank order of variant GB1 surface expression as the immunocytochemical analysis (Ala535Thr > Ala397Val > Glu368Asp > Gly673Asp). The data confirm that transport of the variant receptors assembled with p.Glu368Asp and p.Gly673Asp to the plasma membrane is impaired, while receptors assembled with p.Ala397Val and p.Ala535Thr have close to normal surface expression (Figure 1D). We further determined GABA dose-response curves for WT and mutant GBRs by using an assay based on artificially coupling GBRs via chimeric $G\alpha_{qi}$ proteins to phospholipase C (PLC)[23] (Figure 1A). We monitored PLC activity monitored with a serum responsive element-luciferase (SRE-Luciferase) reporter. Increasing concentrations of GABA yielded sigmoidal dose-response curves for WT and mutant receptors, with the exception of p.Gly673Asp that does not traffic to the cell surface (Figure 1E). p.Glu368Asp exhibited decreased constitutive activity, a reduced Emax, and a nearly 100-fold increased EC50. p.Ala397Val and p.Ala535Thr exhibited a decrease in the Emax but similar constitutive activity and GABA potency as WT receptor. Because the affected individuals are heterozygous for the variations, we also addressed whether co-expression of a variant receptor affects activity of WT receptors (Figure 1E). The data show that the potency of GABA at a mixed population of p.Glu368Asp and WT receptors is significantly decreased versus WTs receptor alone, consistent with the reduced potency of GABA at p.Glu368Asp receptors. In general, the concentration-response curves of mixed populations of variant and WT receptors are similar to those of WT receptors alone, showing that the variant

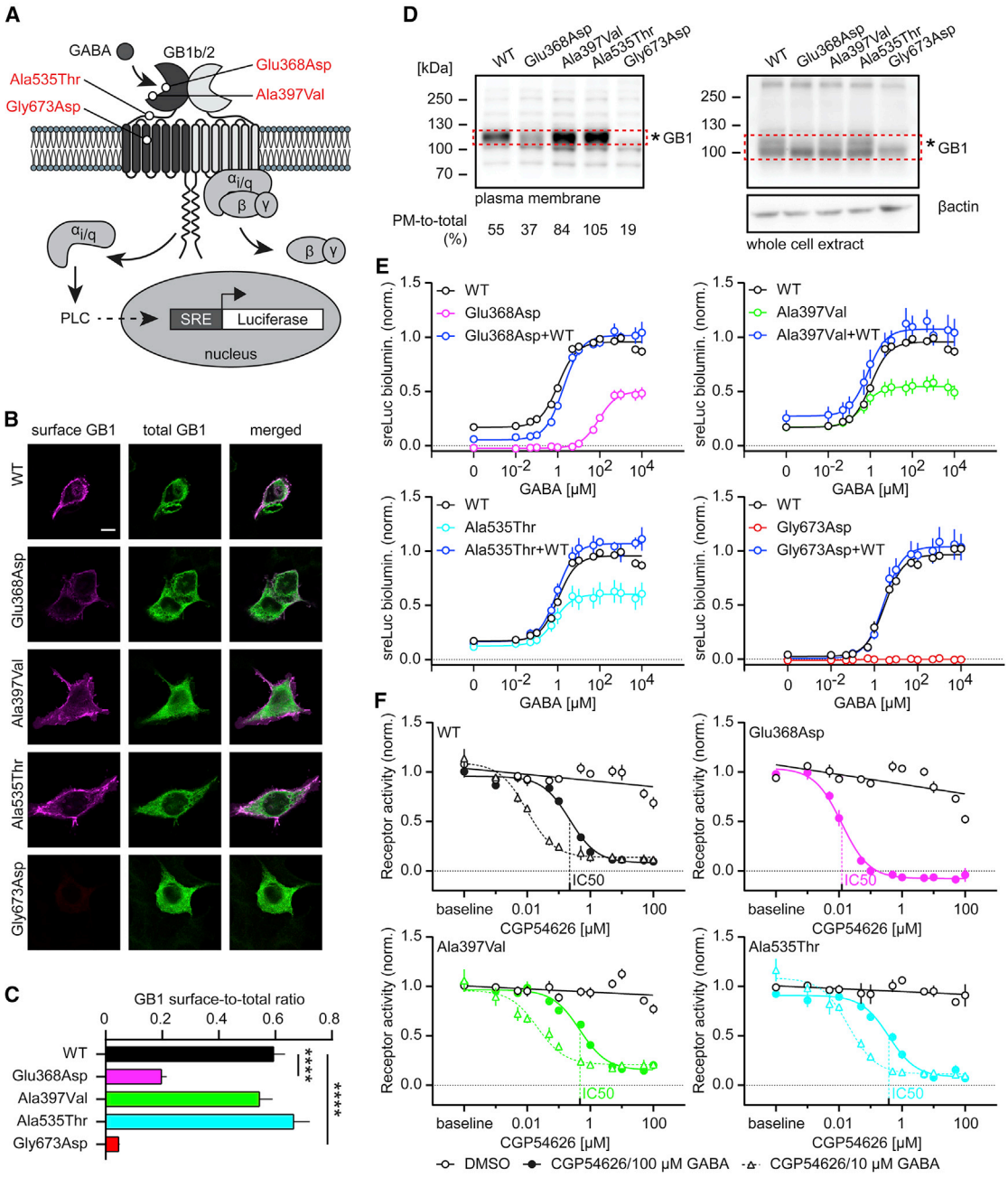

Figure 1. Functional characterization of *de novo* GB1 variants in HEK293 cells

(A) Location of GB1 variants in the heterodimeric GBR. The scheme additionally depicts the assay used to monitor PLC-dependent RLuc expression under control of the serum response element (SRE). GB1b/2 receptors were artificially coupled to PLC by stable expression of the chimeric G protein subunit $G\alpha_{qi}$ in HEK293T cells. GB1b, GB2, and SRE-RLuc were transiently transfected.

(B) Surface and total GB1b expression levels of WT and mutant HA-tagged GB1b subunits co-expressed with GB2 in transfected HEK293 cells. Surface GB1b expression levels were determined with anti-HA antibodies in non-permeabilized cells. Total GB1b expression levels were determined with anti-GB1 antibodies in permeabilized cells. Scale bar: 10 μm.

(C) Bar graphs of the GB1b surface-to-total expression ratio. Kruskal-Wallis ($p < 0.0001$) and Dunn's multiple comparison tests were used because of failed Shapiro-Wilk normality test. ****$p < 0.0001$; WT, n = 28; p.Ala397Val, n = 38; p.Ala535Thr, n = 32; p.Glu368Asp, n = 32; p.Gly673Asp, n = 26.

(D) Fractionation of plasma membrane (PM) proteins in HEK293 cells transiently expressing GB1b/2 receptors. GB1 proteins were identified on immunoblots. WT and variant GB1 protein in the red rectangles was quantified densitometrically. The percentage of PM-to-total GB1 protein is indicated. Immunostaining for β-actin was used to control for loading. The results are from a single experiment. (*) indicates the glycosylated form of GB1. Of note, the loss of glycosylated plasma membrane GB1 protein observed with the p.Glu368Asp and p.Gly673Asp variants is consistent with impaired maturation and surface transport of these proteins.

(E) Dose-response curves showing GABA-induced RLuc activity by WT, variant, and WT+variant (1:1 GB1b plasmid DNA ratio) GBRs in transfected cells. Three parameter log(GABA) versus response nonlinear regression curve fit was used for GABA dose response curves,

(legend continued on next page)

receptors exert no overt dominant-negative effects in heterologous cells. Table S1 provides information about EC50, Emax, and basal activity values derived from the GABA concentration-response curves and the statistical analysis. Inhibition of 10 or 100 μM GABA by increasing concentrations of the GBR antagonist CGP54626 yielded similar IC50 values for WT, p.Ala397Val, and p.Ala535Thr (Figure 1F). The IC50 value of CGP54626 at p.Glu368Asp was decreased, consistent with the lower potency of GABA at this mutant. Table S2 provides IC50 values and the statistical analysis of the CGP54626 inhibition curves.

Discussion

We present here monoallelic *de novo GABBR1* variants that define another gene-Mendelian disease association. Probands with these *de novo* non-synonymous variants all presented developmental and language delays of varying severity. Furthermore, we found an association with hypotonia, intellectual disability, and sleep disorder in two probands and an association with epilepsy in one proband. We note one proband with optic nerve hypoplasia, cortical visual disorders, nystagmus, and hypermetropia.

We analyzed the consequences of the p.Glu368Asp, p.Ala397Val, p.Ala535Thr, and p.Gly673Asp changes for receptor functions in a heterologous expression system monitoring receptor-mediated G protein activation. The alteration of p.Gly673Asp in TM3 renders the receptor completely inactive as a result of lack of receptor expression at the cell surface. Our experiments indicate that p.Gly673Asp does not dimerize with GB2 and therefore does not influence the Emax of co-expressed WT GBRs. The p.Glu368Asp variant is located near the orthosteric binding site and reduces both potency and efficacy of GABA at the receptor. Previous mutagenesis experiments have shown that the neighboring variant p.Tyr367Ala similarly reduces efficacy of GABA,[24] supporting that these variants directly influence the orthosteric binding site and/or trans-subunit conformational changes involved in G protein activation. Surface expression of p.Glu368Asp is impaired, which will further reduce the efficacy of signaling. GABA exhibited normal potency but decreased efficacy at p.Ala397Val and p.Ala535Thr. p.Ala397Val and p.Ala535Thr surface expression is normal, supporting that the two variants affect receptor efficacy by interfering with coupling of agonist binding to G protein activation. Previous mutagenesis experiments showed a similar decrease in agonist efficacy for the p.Trp395Ala variant.[24] All affected individuals harbor monoallelic *de novo* variants of *GABBR1*. We therefore examined whether co-expression of variant and WT GBRs influences the activity of WT receptors in HEK293 cells. The potency of GABA at a mixed population of p.Glu368Asp and WT receptors is significantly reduced versus that of a WT receptor alone, consistent with the reduced potency of GABA at p.Glu368Asp receptors. In general, the concentration-response curves of mixed populations of receptors are similar to those of WT receptors alone, showing that the variant receptors exert no overt dominant-negative effects in heterologous cells. However, in neurons, WT and variant receptors may compete for limiting numbers of synaptic sites as well as trafficking, regulatory, transport, and effector proteins, which could negatively affect WT receptor activity. Therefore, one will have to analyze heterozygous mice harboring the variants to identify possible dominant-negative effects caused by these variants. Overall, our data support that all four variants are loss-of-function mutations that most likely tip the excitation/inhibition balance in the central nervous system towards more excitation, which may explain the epileptiform activity observed with the affected individual with the p.Glu368Asp variant.

Knockout *Gabbr1*$^{-/-}$ and *Gabbr2*$^{-/-}$ mice have been studied for almost 20 years.[2,15,16] These mice lack electrophysiological, biochemical, and behavioral GBR responses. Moreover, they exhibit stereotypical circling, hyperlocomotor activity, delayed sleep phase, frequent seizures, memory deficits, hypothermia, hyperalgesia, hyperactivity, impaired passive avoidance learning, and increased anxiety. Heterozygous *Gabbr1*$^{+/-}$ and *Gabbr2*$^{+/-}$ mice have not been systematically analyzed. Saturation binding experiments with a high-affinity antagonist revealed only an 18% decrease in GBR-binding sites in *Gabbr1*$^{+/-}$ versus *Gabbr1*$^{+/+}$ mice.[16] *Gabbr1*$^{+/-}$ mice showed enhanced prepulse inhibition responses compared to littermate controls, indicating increased sensorimotor gating.[25] This phenotype of *Gabbr1*$^{+/-}$ mice shows that the WT *Gabbr1* allele cannot fully compensate for the loss of GBRs from the knockout allele.

Previous studies[12,13] reported a variety of phenotypes for *GABBR2* variants in affected individuals. They hypothesized that the severity of the phenotypes correlates with the loss of GABA signaling at the variant receptors. Our four *GABBR1*-affected individuals exhibit common phenotypes but differ in disease severity and in associated disorders. Consistent with the level of GBR impairment predicting the severity of the disease, the p.Gly673Asp variant rendering GBRs completely inactive is associated with severe phenotypes, including numerous neurodevelopmental disorders and co-morbid psychiatric disorders. Likewise,

with the exception of p.Gly673Asp, for which a linear regression curve fit was used. Table S1 provides information about EC50, Emax, and basal activity values derived from the GABA concentration-response curves and a statistical analysis.
(F) Dose-response curves showing inhibition of GBR activity (10 μM or 100 μM GABA) by the antagonist CGP54626. Three parameter log(inhibitor) versus response nonlinear regression curve fit was used for CGP54626 dose-response curves and linear regression curve fits for the DMSO controls. The curve fits depict DMSO controls for 100 μM GABA only. All data are mean ± SEM. The number of independent experiments is indicated. Table S2 provides IC50 values and a statistical analysis of the CGP54626 inhibition curves.

Table 2. List of phenotypic features of the four probands

	Individual 1	Individual 2	Individual 3	Individual 4
GABBR1 variant hg19	c.1603G>A (p.Ala535Thr) (GenBank: NM_001470.4)	c.1104G>C (p.Glu368Asp) (GenBank: NM_001470.4)	c.1190C>T (p.Ala397Val) (GenBank: NM_001470.3)	c.2018G>A (p.Gly673Asp) (GenBank: NM_001470.4)
Gender	F	F	M	F
Age	2 years 6 months	4 years 6 months	13 years	17 years
Growth parameters (percentile)				
Head circumference (cm)	P25	P25	P95	P97
Height (cm)	P50–P75	P10–P25	P79	P10–P25
Weight (kg)	P25–P50	P25–P50	P85	P50–P75
Development				
Motor delay	+	+	+	–
Speech delay/abnormalities	+	+	+	+
Hypotonia	+	+	–	–
Repetitive/stereotypical movements	+	–	+ (but resolved with age)	–
Epilepsy	–	+	–	–
Neuropsychiatric problems				
Intellectual disability	not documented	+	+	–
Learning difficulties	not documented	+	+	–
Autism spectrum disorder	–	–	–	+
ADHD	–	–	+	+
Encopresis	–	–	+	–
Sleeping difficulties	–	+	+ (but resolved with age)	+
Ocular	– (note sticky and intense gaze)	+ (optic nerve hypoplasia, cortical visual disorders, intermittent nystagmus, hypermetropia)	–	–
Musculo-skeletal	–	scoliosis	–	congenital bilateral anteversion of femur; bilateral tight heel chord; knee pain
Dermatological	–	–	–	acne vulgaris; xerosis cutis; multiple melanocytic nevi; nail dystrophy

the p.Glu368Asp variant with reduced surface expression, a 100-fold loss in potency, and reduced efficacy is associated with several phenotypes, including epilepsy, severe intellectual disability, ocular problems, and dysmorphic features. The p.Ala397Val and p.Ala535Thr variants, which only exhibit reduced efficacy, produce the mildest phenotypes, mostly characterized by developmental delays. The impairment of GBR functioning caused by the *GABBR1* variants is expected to tip the excitation/inhibition balance in the brain towards increased excitation.[26,27] This is supported by the epileptic phenotype of the individual with the p.Glu368Asp variant. It is surprising that the individual with the p.Gly673Asp variant, which causes a complete loss of GBR function, does not suffer from seizures. We showed that the mutant allele does not interfere with the production of WT receptors from the WT allele, which apparently provides sufficient GBR activity to prevent epileptiform activity.

Baclofen, the GBR agonist marketed for the treatment of muscle pain, spasms, and stiffness in people with multiple sclerosis or spinal cord injury or disease,[1] could be therapeutically used to increase GBR activity in the affected individuals. In this context, baclofen showed promising effects in animal models of *GABBR2*-related Rett syndrome and epileptic encephalopathy.[12] Preclinical and clinical studies are also underway to test the utility of baclofen

for the treatment of ASD[28–30] and epilepsy.[31] In addition, positive allosteric modulators of GBRs are now available.[32,33] Positive allosteric modulators synergistically increase the activity of endogenous GABA at GBRs and allow increasing potency and efficacy of mutant (if still responsive to the modulator) and WT receptors in the affected individuals. Positive allosteric modulators may help to avoid the side-effects experienced with the agonist baclofen, which activates GBRs independent of the presence of endogenous GABA. In addition, treating the individuals with pathogenic *GABBR1* variants with benzodiazepines, which increase GABA inhibition through $GABA_A$ receptors, would also allow for correction of the excitation/inhibition balance.

Data and code availability

The datasets (FASTQ files) supporting the current study have not been deposited in a public repository because of confidentiality of medical diagnostic tests but are available from the corresponding author on request.

Supplemental information

Supplemental information can be found online at https://doi.org/10.1016/j.ajhg.2022.08.010.

Acknowledgments

We thank the families for their participation in the study. This work was supported by the Swiss National Science Foundation (31003A-152970 to B.B.) and the ChildCare Foundation to S.E.A.

Declaration of interests

S.E.A. is a cofounder and CEO of Medigenome, Swiss Institute of Genomic Medicine; he is also a member of the Scientific Advisory Board of the "Imagine Institute", Paris. E.R. is also a cofounder and medical director of Medigenome, Swiss Institute of Genomic Medicine. M.L.C. is an intern in the federally recognized clinical training program for Genetic Medicine of Medigenome. L.N. was supported by the grant NV19-07-00136 from the Ministry of Health of the Czech Republi, and The National Center for Medical Genomics (LM2018132) for support with the WES analyses.

Received: March 28, 2022
Accepted: August 15, 2022
Published: September 13, 2022

References

1. Pin, J.P., and Bettler, B. (2016). Organization and functions of mGlu and GABAB receptor complexes. Nature *540*, 60–68. https://doi.org/10.1038/nature20566.
2. Gassmann, M., and Bettler, B. (2012). Regulation of neuronal GABA(B) receptor functions by subunit composition. Nat. Rev. Neurosci. *13*, 380–394. https://doi.org/10.1038/nrn3249.
3. Favuzzi, E., Huang, S., Saldi, G.A., Binan, L., Ibrahim, L.A., Fernández-Otero, M., Cao, Y., Zeine, A., Sefah, A., Zheng, K., et al. (2021). GABA-receptive microglia selectively sculpt developing inhibitory circuits. Cell *184*, 4048–4063.e32. https://doi.org/10.1016/j.cell.2021.06.018.
4. Mariotti, L., Losi, G., Lia, A., Melone, M., Chiavegato, A., Gómez-Gonzalo, M., Sessolo, M., Bovetti, S., Forli, A., Zonta, M., et al. (2018). Interneuron-specific signaling evokes distinctive somatostatin-mediated responses in adult cortical astrocytes. Nat. Commun. *9*, 82. https://doi.org/10.1038/s41467-017-02642-6.
5. Perea, G., Gómez, R., Mederos, S., Covelo, A., Ballesteros, J.J., Schlosser, L., Hernández-Vivanco, A., Martín-Fernández, M., Quintana, R., Rayan, A., et al. (2016). Activity-dependent switch of GABAergic inhibition into glutamatergic excitation in astrocyte-neuron networks. Elife *5*, e20362. https://doi.org/10.7554/eLife.20362.
6. White, J.H., Wise, A., Main, M.J., Green, A., Fraser, N.J., Disney, G.H., Barnes, A.A., Emson, P., Foord, S.M., and Marshall, F.H. (1998). Heterodimerization is required for the formation of a functional GABA(B) receptor. Nature *396*, 679–682. https://doi.org/10.1038/25354.
7. Kuner, R., Köhr, G., Grünewald, S., Eisenhardt, G., Bach, A., and Kornau, H.C. (1999). Role of heteromer formation in GABAB receptor function. Science *283*, 74–77. https://doi.org/10.1126/science.283.5398.74.
8. Kaupmann, K., Malitschek, B., Schuler, V., Heid, J., Froestl, W., Beck, P., Mosbacher, J., Bischoff, S., Kulik, A., Shigemoto, R., et al. (1998). GABA(B)-receptor subtypes assemble into functional heteromeric complexes. Nature *396*, 683–687. https://doi.org/10.1038/25360.
9. Jones, K.A., Borowsky, B., Tamm, J.A., Craig, D.A., Durkin, M.M., Dai, M., Yao, W.J., Johnson, M., Gunwaldsen, C., Huang, L.Y., et al. (1998). GABA(B) receptors function as a heteromeric assembly of the subunits GABA(B)R1 and GABA(B)R2. Nature *396*, 674–679. https://doi.org/10.1038/25348.
10. Shaye, H., Stauch, B., Gati, C., and Cherezov, V. (2021). Molecular mechanisms of metabotropic GABAB receptor function. Sci. Adv. *7*, eabg3362. https://doi.org/10.1126/sciadv.abg3362.
11. Samanta, D., and Zarate, Y.A. (2019). Widening phenotypic spectrum of GABBR2 mutation. Acta Neurol. Belg. *119*, 493–496. https://doi.org/10.1007/s13760-019-01088-5.
12. Yoo, Y., Jung, J., Lee, Y.N., Lee, Y., Cho, H., Na, E., Hong, J., Kim, E., Lee, J.S., Lee, J.S., et al. (2017). GABBR2 mutations determine phenotype in rett syndrome and epileptic encephalopathy. Ann. Neurol. *82*, 466–478. https://doi.org/10.1002/ana.25032.
13. Vuillaume, M.L., Jeanne, M., Xue, L., Blesson, S., Denommé-Pichon, A.S., Alirol, S., Brulard, C., Colin, E., Isidor, B., Gilbert-Dussardier, B., et al. (2018). A novel mutation in the transmembrane 6 domain of GABBR2 leads to a Rett-like phenotype. Ann. Neurol. *83*, 437–439. https://doi.org/10.1002/ana.25155.
14. Lopes, F., Barbosa, M., Ameur, A., Soares, G., de Sá, J., Dias, A.I., Oliveira, G., Cabral, P., Temudo, T., Calado, E., et al. (2016). Identification of novel genetic causes of Rett syndrome-like phenotypes. J. Med. Genet. *53*, 190–199. https://doi.org/10.1136/jmedgenet-2015-103568.
15. Gassmann, M., Shaban, H., Vigot, R., Sansig, G., Haller, C., Barbieri, S., Humeau, Y., Schuler, V., Müller, M., Kinzel, B., et al. (2004). Redistribution of GABAB(1) protein and atypical GABAB responses in GABAB(2)-deficient mice. J. Neurosci. *24*, 6086–6097. https://doi.org/10.1523/JNEUROSCI.5635-03.2004.
16. Schuler, V., Lüscher, C., Blanchet, C., Klix, N., Sansig, G., Klebs, K., Schmutz, M., Heid, J., Gentry, C., Urban, L., et al. (2001). Epilepsy, hyperalgesia, impaired memory, and loss of pre- and postsynaptic GABA(B) responses in mice lacking

GABA(B(1)). Neuron *31*, 47–58. https://doi.org/10.1016/s0896-6273(01)00345-2.

17. Xi, B., Chen, J., Yang, L., Wang, W., Fu, M., and Wang, C. (2011). GABBR1 gene polymorphism(G1465A)isassociated with temporal lobe epilepsy. Epilepsy Res. *96*, 58–63. https://doi.org/10.1016/j.eplepsyres.2011.04.014.
18. Ma, S., Abou-Khalil, B., Sutcliffe, J.S., Haines, J.L., and Hedera, P. (2005). The GABBR1 locus and the G1465A variant is not associated with temporal lobe epilepsy preceded by febrile seizures. BMC Med. Genet. *6*, 13. https://doi.org/10.1186/1471-2350-6-13.
19. Sobreira, N., Schiettecatte, F., Valle, D., and Hamosh, A. (2015). GeneMatcher: a matching tool for connecting investigators with an interest in the same gene. Hum. Mutat. *36*, 928–930. https://doi.org/10.1002/humu.22844.
20. Kaupmann, K., Schuler, V., Mosbacher, J., Bischoff, S., Bittiger, H., Heid, J., Froestl, W., Leonhard, S., Pfaff, T., Karschin, A., and Bettler, B. (1998). Human gamma-aminobutyric acid type B receptors are differentially expressed and regulate inwardly rectifying K+ channels. Proc. Natl. Acad. Sci. USA *95*, 14991–14996. https://doi.org/10.1073/pnas.95.25.14991.
21. Karczewski, K.J., Francioli, L.C., Tiao, G., Cummings, B.B., Alföldi, J., Wang, Q., Collins, R.L., Laricchia, K.M., Ganna, A., Birnbaum, D.P., et al. (2020). The mutational constraint spectrum quantified from variation in 141, 456 humans. Nature *581*, 434–443. https://doi.org/10.1038/s41586-020-2308-7.
22. Taliun, D., Harris, D.N., Kessler, M.D., Carlson, J., Szpiech, Z.A., Torres, R., Taliun, S.A.G., Corvelo, A., Gogarten, S.M., Kang, H.M., et al. (2021). Sequencing of 53, 831 diverse genomes from the NHLBI TOPMed Program. Nature *590*, 290–299. https://doi.org/10.1038/s41586-021-03205-y.
23. Stefan, E., Aquin, S., Berger, N., Landry, C.R., Nyfeler, B., Bouvier, M., and Michnick, S.W. (2007). Quantification of dynamic protein complexes using Renilla luciferase fragment complementation applied to protein kinase A activities in vivo. Proc. Natl. Acad. Sci. USA *104*, 16916–16921. https://doi.org/10.1073/pnas.0704257104.
24. Geng, Y., Bush, M., Mosyak, L., Wang, F., and Fan, Q.R. (2013). Structural mechanism of ligand activation in human GABA(B) receptor. Nature *504*, 254–259. https://doi.org/10.1038/nature12725.
25. Prosser, H.M., Gill, C.H., Hirst, W.D., Grau, E., Robbins, M., Calver, A., Soffin, E.M., Farmer, C.E., Lanneau, C., Gray, J., et al. (2001). Epileptogenesis and enhanced prepulse inhibition in GABA(B1)-deficient mice. Mol. Cell. Neurosci. *17*, 1059–1070. https://doi.org/10.1006/mcne.2001.0995.
26. Heaney, C.F., and Kinney, J.W. (2016). Role of GABA(B) receptors in learning and memory and neurological disorders. Neurosci. Biobehav. Rev. *63*, 1–28. https://doi.org/10.1016/j.neubiorev.2016.01.007.
27. Lujan, R., and Ciruela, F. (2012). GABAB receptors-associated proteins: potential drug targets in neurological disorders? Curr. Drug Targets *13*, 129–144. https://doi.org/10.2174/138945012798868425.
28. Mahdavinasab, S.M., Saghazadeh, A., Motamed-Gorji, N., Vaseghi, S., Mohammadi, M.R., Alichani, R., and Akhondzadeh, S. (2019). Baclofen as an adjuvant therapy for autism: a randomized, double-blind, placebo-controlled trial. Eur. Child Adolesc. Psychiatry *28*, 1619–1628. https://doi.org/10.1007/s00787-019-01333-5.
29. Erickson, C.A., Veenstra-Vanderweele, J.M., Melmed, R.D., McCracken, J.T., Ginsberg, L.D., Sikich, L., Scahill, L., Cherubini, M., Zarevics, P., Walton-Bowen, K., et al. (2014). STX209 (arbaclofen) for autism spectrum disorders: an 8-week open-label study. J. Autism Dev. Disord. *44*, 958–964. https://doi.org/10.1007/s10803-013-1963-z.
30. Veenstra-VanderWeele, J., Cook, E.H., King, B.H., Zarevics, P., Cherubini, M., Walton-Bowen, K., Bear, M.F., Wang, P.P., and Carpenter, R.L. (2017). Arbaclofen in Children and Adolescents with Autism Spectrum Disorder: A Randomized, Controlled, Phase 2 Trial. Neuropsychopharmacology *42*, 1390–1398. https://doi.org/10.1038/npp.2016.237.
31. Zeman, A., Hoefeijzers, S., Milton, F., Dewar, M., Carr, M., and Streatfield, C. (2016). The GABAB receptor agonist, baclofen, contributes to three distinct varieties of amnesia in the human brain - A detailed case report. Cortex *74*, 9–19. https://doi.org/10.1016/j.cortex.2015.10.005.
32. Kalinichev, M., Girard, F., Haddouk, H., Rouillier, M., Riguet, E., Royer-Urios, I., Mutel, V., Lütjens, R., and Poli, S. (2017). The drug candidate, ADX71441, is a novel, potent and selective positive allosteric modulator of the GABAB receptor with a potential for treatment of anxiety, pain and spasticity. Neuropharmacology *114*, 34–47. https://doi.org/10.1016/j.neuropharm.2016.11.016.
33. Urwyler, S., Mosbacher, J., Lingenhoehl, K., Heid, J., Hofstetter, K., Froestl, W., Bettler, B., and Kaupmann, K. (2001). Positive allosteric modulation of native and recombinant gamma-aminobutyric acid(B) receptors by 2, 6-Di-tert-butyl-4-(3-hydroxy-2, 2-dimethyl-propyl)-phenol (CGP7930) and its aldehyde analog CGP13501. Mol. Pharmacol. *60*, 963–971.

The American Journal of Human Genetics, Volume *109*

Supplemental information

GABBR1 monoallelic *de novo* variants linked to neurodevelopmental delay and epilepsy

Maria Lucia Cediel, Michal Stawarski, Xavier Blanc, Lenka Nosková, Martin Magner, Konrad Platzer, Janina Gburek-Augustat, Dustin Baldridge, John N. Constantino, Emmanuelle Ranza, Bernhard Bettler, and Stylianos E. Antonarakis

GABBR1 Monoallelic *De Novo* Variants Linked to Neurodevelopmental Delay and Epilepsy

Maria Lucia Cediel[1*], Michal Stawarski[2*], Xavier Blanc[1], Lenka Nosková[3], Martin Magner[3,4], Konrad Platzer[5], Janina Gburek-Augustat[6], Dustin Baldridge[7], John N. Constantino[7], Emmanuelle Ranza[1&], Bernhard Bettler[2&], Stylianos E. Antonarakis[1&#]

*****Equal first authors
[&]Joint last authors
[#] Corresponding author

[1] Medigenome, Swiss Institute of Genomic Medicine, 1207 Geneva, Switzerland
[2] Department of Biomedicine, Pharmazentrum, University of Basel, Klingelbergstrasse 50/70, CH-4056 Basel, Switzerland
[3] Department of Pediatrics and Inherited Metabolic Disorders, First Faculty of Medicine, Charles University and General University Hospital in Prague, Czech Republic
[4] Department of Pediatrics, First Faculty of Medicine, Charles University and University Thomayer Hospital in Prague, Czech Republic
[5] Institute of Human Genetics, University of Leipzig Medical Center, Leipzig Germany
[6] Division of Neuropaediatrics, Hospital for Children and Adolescents, University Hospital Leipzig, Germany
[7] Washington University in St. Louis, Missouri, United States of America

Supplementary Data

WES METHODOLOGY

Patient 1

Exome sequencing was performed on the proband and the parents at Genesupport. The capture kit Twist Core Exome and Spike-In were used to capture and enrich the coding regions as well as the splice sites, and the sequencer Illumina NovaSeq 6000 was used as the sequencing platform tool. The sequence were aligned to the human genome reference GRCh37/hg19 using Sentieon (version 201911) and GATK. Finally, using the system Saphethor, the bioninformatic analysis was realized in trio first on a panel of 2113 genes implicated in neurodevelopmental disorders, and then on the totality of the genes covered by the capture kit (8907 genes). The evaluation of the variants was performed using numerous databases including gnomAD (version2.1.1), BRAVO, ClinVar (Version05-Oct-2020), LOVD, local datababses and in silico predictors. Finally, GERP was utilized to determine the conservation of the nucleotides. Confirmation of the variant and family segregation were performed via PCR and Sanger sequencing.

Patient 2

Genomic DNA extracted from leukocytes of the proband and the parents was used for whole-exome sequencing. Exome enrichment was performed on individually barcoded samples using SeqCap EZ MedExome Probes and SeqCap EZ Mitochondrial Genome Design probe (Roche) and sequencing was performed on Novaseq 6000 platform (Illumina) with 100bp paired-end reads. Reads were aligned to the hg19 reference genome using Novoalign version 3.02.13 (Novocraft) with default parameters.

After genome alignment, conversion of SAM format to BAM and duplicate removal was performed using Picard Tools (2.20.8). The Genome Analysis Toolkit, GATK (3.8) (McKenna et al., 2010) was used for local realignment around indels, base recalibration, variant recalibration, and variant calling. Variants were annotated using the GEMINI framework (Paila et al., 2013) and filtered based on the population frequencies using several public databases and an in-house database of population-specific variants. Identification of candidate variants was performed for autosomal dominant (de novo variants) and autosomal recessive inheritance patterns. Variants were further prioritized according to the functional impact and conservation score. Sanger sequencing confirmed the presence of the candidate.

McKenna A, Hanna M, Banks E, Sivachenko A, Cibulskis K, Kernytsky A, et al. The Genome Analysis Toolkit: a MapReduce framework for analyzing next-generation DNA sequencing data. Genome Res 2010; 20: 1297-303.

Paila U, Chapman BA, Kirchner R, Quinlan AR. GEMINI: integrative exploration of genetic variation and genome annotations. PLoS Comput Biol 2013; 9: e1003153.

Patient 3

The exome capture was carried out with BGI Exome kit capture (59M) and the library was then sequenced on a BGISEQ-500, paired-end 100bp. Analysis of the raw data was performed using the software Varfeed (Limbus, Rostock) and the variants were annotated and prioritized using the software Varvis (Limbus, Rostock). All potential protein-influencing variants were prioritized with regard to their pathogenicity and clinical relevance according to all possible inheritance modes. On an exploratory base, CNV analysis of down to single exon deletion was performed. Coverage of more than 20x was been achieved in more than 95 % of target sequences in all family members.

Patient 4

Clinical exome sequencing was performed at GeneDx according to previously described methods (Retterer et al., 2016). Briefly, genomic DNA was obtained from the proband and parents, exonic regions and nearby splice junctions were captured and sequenced with 100bp or larger paired-end reads. Alignment was done with human genome build GRCh37/UCSC hg19, and Xome Analyzer, a custom analysis tool, was used for analysis. All potentially pathogenic variants were confirmed via capillary sequencing or another appropriate method.

Retterer K, Juusola J, Cho MT, Vitazka P, Millan F, Gibellini F, et al., Clinical application of whole-exome sequencing across clinical indications. Genet Med. 2016 Jul;18(7):696-704.

Figure S1

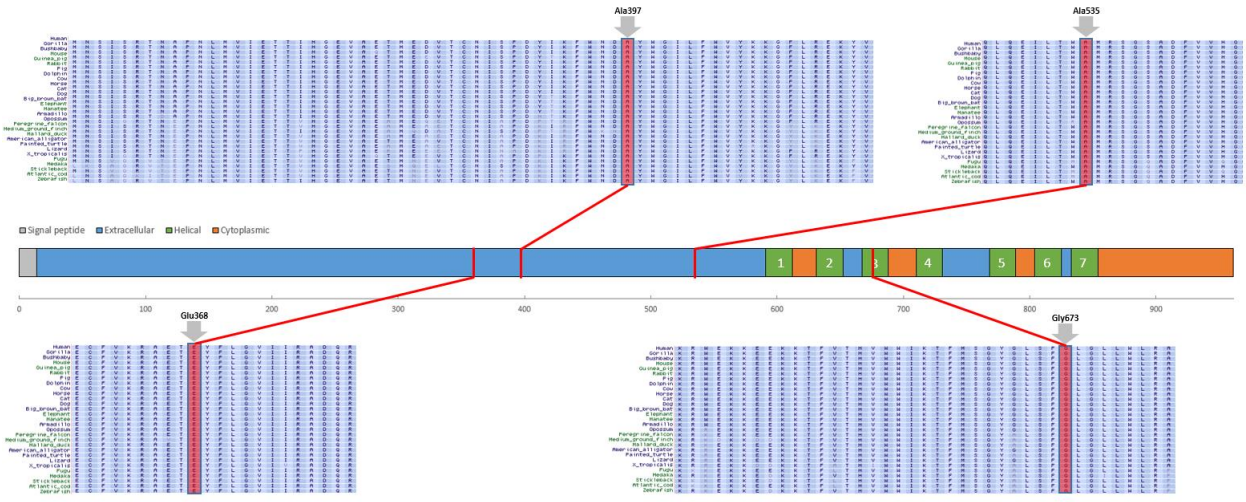

Figure S1. Evolutionary conservation of the four GABBR1 *de novo* variants. The cartoon of the primary structure of the GABBR1 protein is shown in the middle (the scale below depicts the number of aminoacids). The 7 transmembrane domains are numbered and shown in green. The aminoacids

shown with arrows are mutated in the patients studied. The species shown are depicted in the left of each panel.

Table S1. Parameters of GABA concentration-response curves fitted to the raw data in Fig. 1e

	WT	Glu368Asp	WT+Glu368Asp		*WT & Glu368Asp*	*WT & WT+Glu368Asp*	*Glu368Asp & WT+Glu368Asp*
basal	0.17	-0.02	0.05	*Kruskal-Wallis (p<0.0001) & Dunn's*	*p<0.0001*	*p=0.3938*	*p=0.2597*
Emax	0.96	0.50	1.02	*ANOVA (p<0.0001)/Games-Howell's*	*p<0.0001*	*p=0.5754*	*p<0.0001*
EC50 [µM]	1.12	91.88	1.88	*ANOVA (p<0.0001)/Holm-Sidak's*	*p<0.0001*	*p<0.0001*	*p<0.0001*
n	15	13	4				
	WT	Ala397Val	WT+Ala397Val		*WT & Ala397Val*	*WT & WT+Ala397Val*	*Ala397Val & WT+Ala397Val*
basal	0.17	0.17	0.27	*ANOVA (p=0.2954)/Tukey's*	*p=0.9996*	*p=0.3001*	*p=0.2995*
Emax	0.96	0.55	1.08	*ANOVA (p=0.0003)/Holm-Sidak's*	*p<0.0001*	*p=3702*	*p=0.0153*
EC50 [µM]	1.12	0.61	0.82	*ANOVA (p=0.0003)/Tukey's*	*p=0.0002*	*p=0.2026*	*p=0.4708*
n	15	17	4				
	WT	Ala535Thr	WT+Ala535Thr		*WT & Ala535Thr*	*WT & WT+Ala535Thr*	*Ala535Thr & WT+Ala535Thr*

basal	0.17	0.12	0.17	*Kruskal-Wallis (p=0.3985) & Dunn's*	*p=0.6735*	*p>0.9999*	*p>0.9999*
Emax	0.96	0.60	1.07	*ANOVA (p=0.0004)/Games-Howell's*	*p=0.0085*	*p=0.3528*	*p=0038*
EC50 [µM]	1.12	0.80	0.94	*ANOVA (p=0.0275)/Tukey's*	*p=0.0208*	*p=0.5664*	*p=0.7254*
n	15	17	4				
	WT	Gly673Asp	WT+Gly673Asp		*WT & Gly673Asp*	*WT & WT+Gly673Asp*	*Gly673Asp & WT+Gly673Asp*
basal	0.02	-0.01	0.01	*t-test*		*p=0.4471*	
Emax	0.97	0	1.04	*t-test with Welch's correction*		*p=0.5784*	
EC50 [µM]	3.35	-	3.04	*t-test with Welch's correction*		*p=0.5830*	
n	12	10	16				

Table S2. IC50 values for CGP54626 dose response curves fitted to the raw data in Fig. 1f

IC50 [µM]	WT	Glu368Asp	Ala397Val	Ala535Thr
@ 10 µM GABA (n=3*)	0.01	0.01	0.02	0.02
@100 µM GABA (n=6)	0.24	0.01	0.50	0.41
@100 µM GABA t-test WT vs.		*0.0002*	*0.0027*	*0.0116*
		Welch's correction		

*Glu368Asp: n=2 (ambiguous fit)